Capítulo 4

Mathematical Model of a Rotor-Bearing System and the Passive Control

Álvaro Cabrera Amado[1]
Gerardo Silva Navarro[2]
Manuel Arias Montiel[3]
Rafael Castillo Rincón[4]

Abstract: This paper presents a mathematical model of a rotor-bearing system and the vibration control using a passive absorber. The system with the passive absorber is modeled using Finite Element Methods (FEM). The primary system consists in a rotor system mounted on two supports at its ends, one of them is a classical journal bearing and the other one is a bearing on a slider which can be displaced in order to change the distance between supports. The passive absorber is a concentrated mass mounted at the end of a cantilever beam which is an extension of the flexible shaft of the rotor system. The vibration attenuation in the rotor system is achieved modifying the system dynamics by the displacement of the slider bearing which causes changes in the absorber and primary system stiffness and as a consequence in their natural frequencies. To control the slider bearing position a PD control scheme is used, which is parameterized in terms of the angular speed of rotor. Some numerical simulations are included to illustrate the dynamic performance, obtaining reductions up to 80% in the unbalance response of the primary system.

[1]alvaroca_1@hotmail.com. Departamento de Mecatrónica, Universidad del Papaloapan.

[2]gsilva@cinvestav.mx. Departamento de Ingeniería Eléctrica, Sección de Mecatrónica, Centro de Investigación y de Estudios Avanzados del Instituto Politécnico Nacional.

[3]mam@mixteco.utm.mx. Departamento de Mecatrónica, Universidad Tecnológica de la Mixteca.

[4]rafascast2@hotmail.com. Departamento de Mecatrónica, Universidad del Papaloapan.

Resumen: Este artículo presenta el modelo matemático de un sistema rotor-chumacera y el control de vibración usando un absorbedor pasivo. El sistema es modelado mediante los métodos de elementos finitos (FEM). El sistema primario consiste en un rotor montado sobre dos soportes en sus extremos, uno de ellos es una clásica chumacera con baleros y la otra es una chumacera sobre guías lineales, los cuales pueden ser desplazados para cambiar la distancia entre los soportes. El absorbedor pasivo está formado por una masa concentrada en el extremo de una viga en voladizo, el cual es una extensión de la flecha del rotor. La cancelación de vibración en el sistema se logra modificando la dinámica del sistema mediante el desplazamiento de la chumacera móvil, ésta produce cambios en el absobedor y rigidez del sistema primario y como consecuencias produce cambios en la frecuencia natural del sistema. El movimiento de la chumacera se realiza mediante un esquema de control PD, el cual está en función de la velocidad angular del rotor. El trabajo presenta resultados numéricos, la respuesta en el desbalance se reduce cerca del 80% en el sistema primario.

Palabras clave: Suspensión semiactiva de vehículo, Amortiguador magnetorreológico, Control Modal, Absorción de vibraciones.

4.1   Introduction

Vibration control in structures and machines has been a field of interest in varied branches of engineering, technology and industry for many years. The three most commonly used classification of vibration control systems are: passive, active and semi-active. Active and semi-active controllers require external power sources while the passive ones do not require external power for their operation. Active and semi-active control schemes in rotordynamics have been widely studied [Zhou2001], [Forte2004]. In contrast, a vibration absorber is a mass-spring system with very little or no damping, which can absorb vibration excitations through energy transfer into it, thereby reducing the vibrations of the primary system [DeSilva1999]. Passive control of vibration is relatively simple and straightforward, robust,reliable and economical, but it has its limitations, namely, it is not possible to adjust the control forces once the device is designed and implemented. Therefore, this kind of vibration control systems are designed and performed for some specific frequencies.

Recently, vibration absorbers have been modified in order to improve their performance in a more wide frequency range with applications in structures. Chen & Wang [Chen2004] propose to use of mass-damper systems along a simply supported Timoshenko beam to reduce the vibrations of the first mode shapes, they present only numerical results for this method.

Blanco *et al.* [Blanco2003] propose a Jeffcott-like rotor supported on two bearings, one of which can be horizontally moved, by means of some servomechanism in order to compensate the system response. The asymmetric motion of the disk, because of the motion of one of the supporting bearings, leads to a nonlinear and coupled model. The proposed methodology for dynamic stiffness control of the transient run-up of the rotor consists of two controllers: the first one, is a controller for the trajectory planning for the speed trajectory, and the second one, is a controller for the smooth switching on the position of the movable bearing. This technique allows to reduce and stabilize the unbalance response while passing through its first critical speed.

Jalili & Knowles [Jalili2004] present an active resonator absorber for structural vibration control showing its effectiveness and stability by numerical simulations and proposing an inertial piezoelectric actuator for future applications. Sun *et al.* [Sun2007] shows a new kind of adaptive active resonator absorber which combines an adaptive passive vibration absorber with an active resonator absorber getting a reduction in the control effort observed by numerical results.

The works above mentioned apply vibration absorbers in structures. In this paper we propose an absorber to be used in a rotor-bearing system in order to attenuate its unbalance response. For this, the primary system and the absorber dynamics are modified by the displacement of one of the rotor supports, which is mounted on a slider. This motion is parameterized in terms of the spin speed of the rotor such that the slider tracks certain trajectory to avoid the resonant peaks and in this way reduce the unbalance response during the running up. Some numerical results show a good closed loop performance in comparison with the open loop system, obtaining reductions in vibration amplitudes up to 84%.

4.2 Rotor-bearing system with passive absorber

The primary system consists in a rotor system mounted on two supports at its ends, one of them is a classical journal bearing and the other one is a journal bearing on two sliders. A plane disk with mass m_r is mounted on the flexible shaft of the rotor, it is supported in the left by a traditional journal bearing which is rigid enough with large stiffness k_{iy} and the right journal bearing is mounted

on two sliders to change the distance between supports into some small interval, which provides the appropriated longitudinal force to reduce vibrations of the primary system.

The rotor has a cantilever beam absorber, which is an extension of the flexible shaft of the rotor-bearing system. It has a concentrated mass m_a mounted on a ball bearing at the shaft end (this mass does not rotate). For regulation of the angular speed ω is considered a CD motor, which is controlled by a speed driver with an internal PID control (see Fig. 4.1).
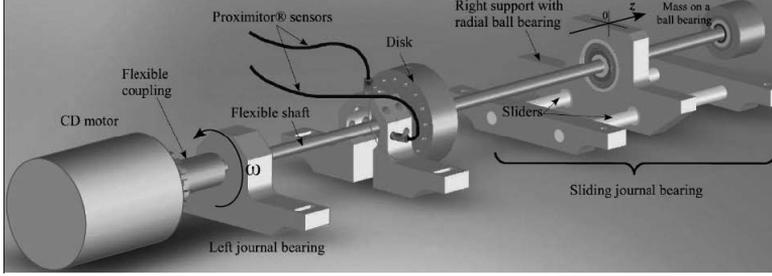
Figura 4.1: Rotor-bearing system with a cantilever beam absorber.

4.3   Rotor-bearing model

The rotor is modeled using finite element methods, where three finite elements and four nodes are considered to construct the reduced model of the rotor-bearing system. The schematic diagram of the discretized model is shown in Fig. 4.2. Both journal bearings have different dynamics, with mass, stiffness and viscous damping. The finite elements have lengths $l_1, l_2,$ and l_3, material density ρ, transversal section A, moment of inertia I and Young's modulus E for the isotropic elastic shaft.

The mathematical model is analyzed in one plane of motion for the vertical y dynamics. The FEM model assumes that each journal bearing has concentrated mass and stiffness in the corresponding nodes on the beam. The viscous damping in the rotor is considered proportional to the mass and stiffness. The finite elements are considered as Euler type beam and each element has 2 DOF per node as illustrated in Fig. 4.2.

Here the vertical displacement of the disk is y_r, the unbalance mass in the disk m_r and the disk eccentricity e. The left journal bearing has radial displacement y_i, a mass m_i and the stiffness is approximated by k_{iy}. The sliding journal bearing has radial displacement y_d, the linear displacement z, its mass m_d and its stiffness is approximated by a large value k_{dy}. The passive absorber is a cantilever like-beam that has a concentrated mass m_a mounted on a ball bearing at the shaft end (this mass does not rotate).

Figura 4.2: Schematic diagram of the discretized rotor-bearing system.

The angular deflections of the beam are represented by coordinates, β_{iy} in the left journal bearing , β_{ry} in the disk, β_{dy} to the right journal bearing and β_{ay} at the shaft end (see Fig. 4.2).

For the beam absorber is considered 2 DOF per each node, such that the overall model has 8 DOF , and an additional degree corresponding to the linear displacement of the sliding journal bearing. The beam model is endogenously perturbed by the unbalance force f_y due to the unbalance mass m_r in the disk.

The mass, stiffness and damping elemental matrices for the finite element model of a rotor-bearing systems are based in Genta [Genta2005].

The stiffness matrix K_y of the rotor-bearing is given by:

$$
K_y = EI
\begin{bmatrix}
\frac{12}{l_1^3}+\frac{k_{iy}}{EI} & \frac{6}{l_1^2} & -\frac{12}{l_1^3} & \frac{6}{l_1^2} & 0 & 0 & 0 & 0 \\
& \frac{4}{l_1} & -\frac{6}{l_1^2} & \frac{2}{l_1} & 0 & 0 & 0 & 0 \\
& & \frac{12}{l_1^3}+\frac{12}{l_2^3} & \frac{6}{l_2^2}-\frac{6}{l_1^2} & -\frac{12}{l_2^3} & \frac{6}{l_2^2} & 0 & 0 \\
& & & \frac{4}{l_1}+\frac{4}{l_2} & -\frac{6}{l_2^2} & \frac{2}{l_2} & 0 & 0 \\
& & & & \frac{12}{l_2^3}+\frac{12}{l_3^3}+\frac{k_{dy}}{EI} & \frac{6}{l_3^2}-\frac{6}{l_2^2} & -\frac{12}{l_3^3} & \frac{6}{l_3^2} \\
& & \text{sym} & & & \frac{4}{l_2}+\frac{4}{l_3} & -\frac{6}{l_3^2} & \frac{2}{l_3} \\
& & & & & & \frac{12}{l_3^3} & -\frac{6}{l_3^2} \\
& & & & & & & \frac{4}{l_3}
\end{bmatrix}
$$

The mass matrix M_y is:

$$M_y =$$

$$
\frac{\rho A}{420}
\begin{bmatrix}
156l_1+m_i\frac{420}{\rho A} & 22l_1^2 & 54l_1 & -13l_1^2 & 0 & 0 & 0 & 0 \\
& 4l_1^3 & 13l_1^2 & -3l_1^3 & 0 & 0 & 0 & 0 \\
& & a_{33} & 22l_2^2-22l_1^2 & 54l_2 & -13l_2^2 & 0 & 0 \\
& & & 4l_1^3+4l_2^3 & 13l_2^2 & -3l_2^3 & 0 & 0 \\
& & & & a_{55} & 22l_3^2-22l_2^2 & 54l_3 & -13l_3^2 \\
& & \text{sym} & & & 4l_2^3+4l_3^3 & 13l_3^2 & -3l_3^3 \\
& & & & & & a_{77} & -22l_3^2 \\
& & & & & & & 4l_3^3
\end{bmatrix}
$$

$$
a_{33}=156l_1+156l_2+m_r\frac{420}{\rho A},\; a_{55}=156l_2+156l_3+m_d\frac{420}{\rho A},\; a_{77}=156l_3+m_a\frac{420}{\rho A}
$$

The proportional damping matrix is a linear combination

$$C_y = 19.1 M_y + 18 \times 10^{-6} K_y$$

The dynamics of the sliding journal bearing is assumed as follows

$$m_d \ddot{z} + c_d \dot{z} = u \tag{4.3.1}$$

where u denotes the control force.

The global system vertical dynamics is described as:

$$M\ddot{q} + C\dot{q} + Kq = Bu + F(t) \qquad\qquad M, C, K \in R^{9 \times 9} \tag{4.3.2}$$

$$M = \begin{bmatrix} M_y & 0 \\ 0 & m_d \end{bmatrix}; \quad C = \begin{bmatrix} C_y & 0 \\ 0 & c_d \end{bmatrix}; \quad K = \begin{bmatrix} K_y & 0 \\ 0 & 0 \end{bmatrix}$$

$$q = \begin{bmatrix} y_i & \beta_{iy} & y_r & \beta_{ry} & y_d & \beta_{dy} & y_a & \beta_{ay} & z \end{bmatrix}^T$$

$$B = \begin{bmatrix} 0 & 0 & 0 & 0 & 0 & 0 & 0 & 0 & 1 \end{bmatrix}^T$$

$$F(t) = \begin{bmatrix} 0 & 0 & f_y(t) & 0 & 0 & 0 & 0 & 0 & 0 \end{bmatrix}^T$$

$$f_y(t) = m_r e \omega^2 \sin \omega t - m_r e \dot{\omega} \cos \omega t$$

The physical parameters for the overall 9 DOF rotor-bearing system are given in Table I.

Table I. Rotor-bearing system parameters		
Left journal bearing	Disk and absorber	Right journal bearing
$m_i = 0.4\,kg$	$m_r = 0.808\,kg$	$m_d = 0.4\,kg$
$k_{iy} = 4 \times 10^4 \frac{kN}{m}$	$m_a = 0.6505\,kg$	$k_{dy} = 4 \times 10^4 \frac{kN}{m}$

Other parameters of the system are: Young's modulus $E = 200\,GPa$, total length of the shaft $L = 0.512\,m$, first finite element length $l_1 = 0.19\,m$, second element length $l_2 = 0.19 + z$, third element length $l_3 = 0.1322 - z$, eccentricity $e = 43\mu m$, shaft diameter $D = 0.01\,m$, material density $\rho = 7807\,\frac{kg}{m^3}$, inertia moment $I = \pi D^4/64$, transversal section $A = \pi D^2/4$, and the coordinate z can be moved into the range $[-0.06, ..., 0.06]\,m$.

4.4   Natural frequencies of the Rotor Model

The natural frequencies are obtained from the undamped mathematical model (4.3.2) in free vibrations as:

$$M\ddot{q} + Kq = 0, \quad q \in R^9 \tag{4.4.1}$$

The natural frequencies associated with the vibration modes of the system are the eigenvalues of $M^{-1}K$ and two main natural frequencies are shown in Fig. 4.3(a), when the sliding journal bearing is moved into the range $\{-0.05, ..., 0.05\}\, m$. The first natural frequency ω_{n1} is associated to the disk m_r and the second ω_{n2} to the mass m_a at the shaft end.
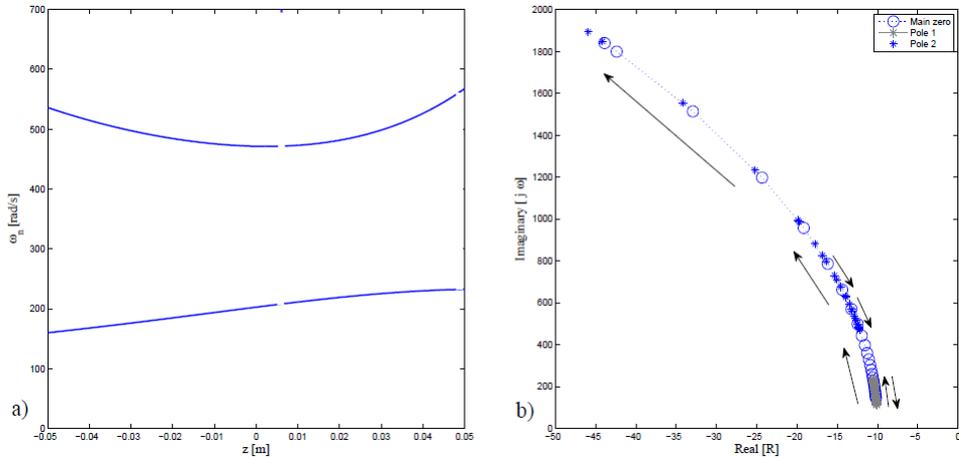
Figura 4.3: (a)The natural frequencies change their values, when the sliding journal bearing is moved, (b) Main zero and two poles are shown for z into the range $[-0.13, ..., 0.12]\, m$.

The main poles and zero change their values, when the sliding journal bearing is moved into the range $[-0.13, ..., 0.12]\, m$ (see Fig. 4.3(b)). They are obtained of the transfer function $G(s) = \frac{y_r(s)}{f_y(s)}$ and their numerical values are represented in Fig.4.3(b).

4.5 Results for different positions z

Consider the overall rotor-bearing system (4.3.2), whose parameters are given in Table I. The initial conditions in the rotor-bearing system are $y_i(0) = y_r(0) = y_d(0) = y_a(0) = 0\, m$ and the initial position of the sliding support $z(0) = -0.04\, m$. Fig. 4.4(a) shows the open-loop unbalance response of the disk y_r for different positions z, when the rotor run-up is started from 0 to $4000\, rpm$ $(418.879\, \frac{rad}{s})$ during $30\, s$. The results show how the dynamics of the rotor-bearing system change for different positions of the sliding support, mainly its dynamic stiffness contributes to modify the natural frequencies and, then the overall system dynamics is modified.

When the shaft length between supports is longer, the vertical displacement of the disk is incremented. This is due to cantilever beam absorber length is reduced and then the passive absorber loses the vibration absorption capacity in
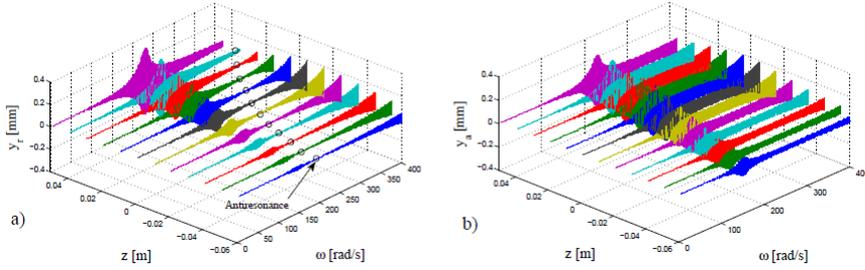
Figura 4.4: (a) Vertical displacements of the disk y_r for different positions of sliding journal bearing $z = \{-0.06, ..., 0.05\} \, m$, and (b) displacements of the mass at the shaft end y_a.

the primary system as shown in Fig. 4.4(b).

4.6   Semiactive unbalance compensation

For the application, we consider the rotor-bearing system (4.3.2), which is uncontrollable from the sliding journal bearing position. For the sliding support position regulation is implemented a PD control scheme as follows:

$$u = -\alpha_1(z - z^*) - \alpha_2(\dot{z} - \dot{z}^*) \tag{4.6.1}$$

$$z^*(\omega) = p_1\omega^2 + p_2\omega + p_3 \tag{4.6.2}$$
$$p_1 = -8.572 \times 10^{-6}, \, p_2 = 3.078 \times 10^{-3}, \, p_3 = -0.4177$$

and z^* denotes the desired position of the sliding journal bearing, which is parameterized in terms of the antiresonance frequencies. These frequencies are associated to zeros of the transfer function $G(s) = \frac{y_r(s)}{f_y(s)}$ in the rotor-bearing system. The vibrations of the overall system are synchronous, meaning that the vibration frequency is identical to the motor angular speed ω (see Figs. 4.4(a) and 4.3(b)). The desired position z^* is saturated between -0.06 and $0.06 \, m$. The design parameters of the PD control to regulate the sliding support position are selected as $\alpha_1 = 1000$, $\alpha_2 = 990$.

The sliding journal bearing is moved according to z^*, which is based on the antiresonance frequencies ω of the system and the optimal trajectory to follow is shown in Fig. 4.4(a). To apply the PD control scheme the measurements of the angular speed ω and the linear displacement of the sliding journal bearing z are necessary. The vibration absorption in the primary system is shown in Fig. 4.5(a).

In Fig. 4.6 is shown the controllable position of the sliding support and the linear force to move it, which is contained between -0.4 and $0.4 \, N$.
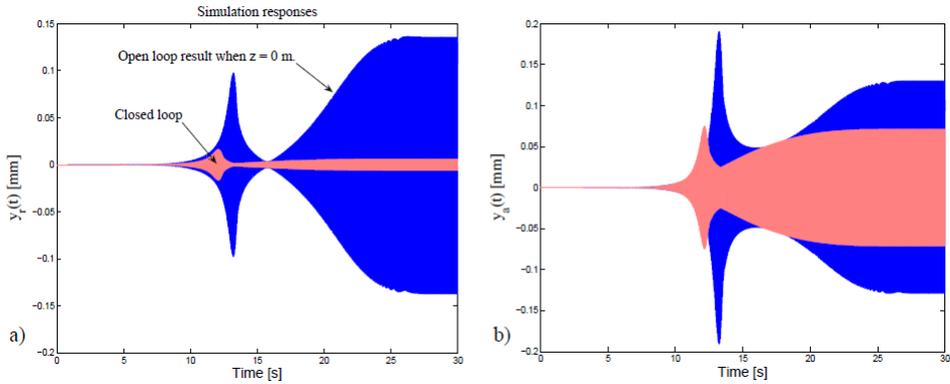
Figura 4.5: (a) Closed loop response of the disk m_r, and b) displacement at the shaft end m_a.
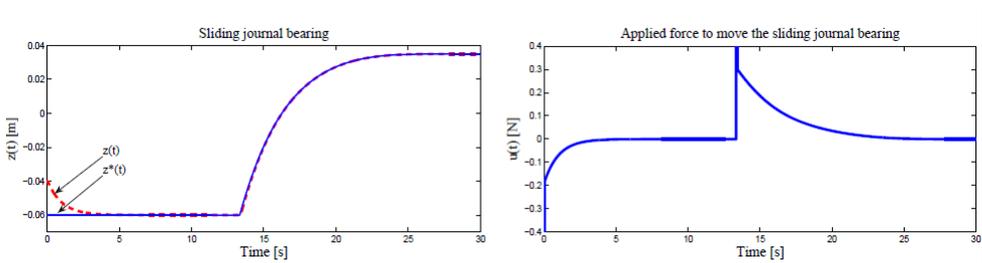
Figura 4.6: Controllable position of sliding journal bearing $z(t)$.

4.7 Conclusions

In this work a 9 DOF model for a rotor-bearing system with a cantilever beam absorber is addressed. The passive absorber allows to reduce the vibrations due the unbalance mass of the disk by controlling its dynamic stiffness. To reduce the vibrations of the primary system is only needed to move the sliding journal bearing in terms of the angular speed into a specific range. The natural frequency of the cantilever beam absorber changes when the sliding journal bearing changes of position on two sliders. This simple technique allows to absorb vibrations of the overall rotor-bearing system, when passing through the first critical speed or natural frequency associated to the disk. The unbalance response of the disk is reduced up to 80% with respect to the open-loop response.

Bibliografía

[Blanco2003] Blanco-Ortega, A., Silva-Navarro, G. & Gómez-Mancilla, J. C. 2003. **Dynamic Stiffness Control and Acceleration Scheduling for the Active Balancing Control of a Jeffcott-Like Rotor System**. Proc. The 10th International Congress on Sound and Vibration, pp. 227-234, July, Stockholm.

[Chen2004] Chen, Y-H. & Huang, Y-H. 2004. **Timoshenko beam with tuned mass dampers and its design curves**. Journal of Sound and Vibrationl, vol. 278, pp. 873-888, 2004.

[DeSilva1999] De Silva, C. W. 1999. **Vibration: fundamentals and practice**. CRC Press, USA.

[Forte2004] Forte, P., Paterno, M. & Rustighi, E. 2004. **A magnetorheological fluid damper for rotor applications**. International Journal of Rotating Machinery, Vol. 10, No. 3, pp. 175-182.

[Genta2005] Genta, G. 2005 **Dynamics of Rotating Systems**. Springer-Verlag, NY.

[Inman2006a] Inman, D.J. 2006. **Vibration with Control**. John Wiley & Sons, Ltd. Academic Press, England.

[Inman2006b] Inman, D.J., Tarazaga, P. A. & Salehian, A. 2006. **Active and passive damping of structures**. Proc. of the 13th Int. Congress on Sound and Vibration (ICSV13), July 2-6, Vienna, Austria.

[Jalili2004] Jalili, N., & Knowles, D. W. 2004. **Structural vibration control using an active resonator absorber: modeling and control implementation**. Smart Materials ans Structures, Vol. 13, pp. 998-1005.

[Sun2007] Sun, H. L., Zhang, X. L., Gong, X. L. & Chen, H. B. 2007. **A novel kind of active resonator absorber and the simulation of its control effort**. Journal of Sound and Vibration, Vol. 300, pp. 117-125.

[Vance1988] Vance, J.M. 1988. **Rotordynamics of Turbomachinery**. John Wiley & Sons, NY.

[Zhou2001] Zhou, S. & Shi, J. 2001. **Active balancing and vibration control of rotating machinery: A survey**. The Shock and Vibration Digest, Vol. 33, No. 4, pp. 361-371.